Nanoparticle protein corona-enabled biomarker discovery to differentiate bacterial sepsis from non-infectious acute systemic inflammation

Lana Papafilippou,[a] Andrew Claxton,[b] Paul Dark,[b,c] Marilena Hadjidemetriou*[a] and Kostas Kostarelos*[a]

[a]*Nanomedicine Lab, Faculty of Biology, Medicine & Health, AV Hill Building, The University of Manchester, Manchester, M13 9PT, UK*

[b]*Centre for Acute Care Trauma, Manchester Academic Health Science Centre, Health Innovation Manchester, Division of Critical Care, Salford Royal NHS Foundation Trust, Greater Manchester, UK*

[c]*Division of Infection, Immunity and Respiratory Medicine, Faculty of Biology, Medicine & Health, AV Hill Building, The University of Manchester, Manchester, M13 9PT, UK.*

* Correspondence should be addressed to: marilena.hadjidemetriou@manchester.ac.uk; kostas.kostarelos@manchester.ac.uk

Abstract

Rapid and accurate diagnosis of sepsis remains clinically challenging. The lack of specific biomarkers that can differentiate sepsis from non-infectious systemic inflammatory diseases often leads to excessive antibiotic treatment. Novel diagnostic tests are urgently needed to rapidly and accurately diagnose sepsis and enable effective treatment. Despite investment on cutting-edge technologies available today, the discovery of disease-specific biomarkers in blood remains extremely difficult. The highly dynamic environment of blood restricts access to vital diagnostic information that can be obtained by proteomic analysis. Here, we employed clinically used lipid-based nanoparticles (AmBisome®) as an enrichment platform to analyze the human plasma proteome in the setting of sepsis. We exploited the spontaneous interaction of plasma proteins with nanoparticles (NPs) once in contact, called the 'protein corona', to discover previously unknown disease-specific biomarkers for sepsis diagnosis. Plasma samples obtained from non-infectious acute systemic inflammation controls and sepsis patients were incubated *ex vivo* with AmBisome® liposomes, and the resultant protein coronas were thoroughly characterised and compared by mass spectrometry (MS)-based proteomics. Our results demonstrate that the proposed nanoparticle enrichment technology enabled the discovery of 67 potential biomarker proteins that could reproducibly differentiate non-infectious acute systemic inflammation from sepsis. This study provides proof-of-concept evidence that nanoscale-based 'omics' enrichment technologies have the potential to substantially improve plasma proteomics analysis and to uncover novel biomarkers in a challenging clinical setting.

Keywords: sepsis, infectious disease, inflammation, nanomedicine, biomarkers, liposomes

Introduction

Sepsis is defined as a life-threatening organ dysfunction triggered by a dysregulated immune response to an infection.[1] It is a leading cause of mortality, accounting for more than six million deaths each year worldwide.[2] Delays in diagnosing sepsis and initiating appropriate antimicrobial treatments are associated with higher mortality.[3] Hence, there is an unmet need for the development of biomarkers to rapidly diagnose sepsis and monitor its progression.

A significant challenge in the clinical setting is the diagnostic uncertainty in differentiating patients with sepsis in a highly heterogeneous, critically ill patient population. Microbiological cultures are the current gold standard for identifying causative pathogen phenotypes and guiding antimicrobial treatment,[4] however they are limited by a lack of sensitivity and by long incubation times (up to 72 hours).[5] Given the high mortality rate associated with delayed treatments and the lack of specific diagnostic tools, broad-spectrum antimicrobial treatment is recommended in all patients suspected of developing sepsis.[6] As a result, broad-spectrum antimicrobials are frequently administered to patients with acute sterile inflammation or viral infections, contributing to the emergence and propagation of antimicrobial resistant pathogens.[7] Blood-circulating C-reactive protein and procalcitonin biomarkers are increasingly used in routine clinical practice to help identify unwell patients,[8, 9] yet they lack diagnostic specificity as they are known to be upregulated in other acute inflammatory disorders.[10, 11]

Considering the complexity of the sepsis syndrome and the molecular pathways underlying immune responses that can also arise from non-infectious diseases,[12] the use of a single diagnostic biomarker is unlikely to offer the required specificity and sensitivity.[13] To date, the lack of protein biomarkers or biomarker combinations to identify sepsis is partially attributed to the incapacity of currently available proteomics platforms to offer an in-depth analysis of the plasma proteome.[14]

Although nanotechnology-based platforms have been developed to enable the quantification of specific blood molecules, ongoing efforts are focusing on the discovery of previously undetectable disease-specific biomarkers.[15] We have previously exploited the spontaneous interaction of intravenously administered nanoparticles with proteins, named the 'protein corona',[16, 17] to capture and amplify low molecular weight and low abundant proteins from the blood circulation of tumour-bearing mice and ovarian carcinoma patients.[18, 19] The protein corona formed around intravenously injected clinically-used liposomes was found to be enriched with disease-specific proteins which could not be detected by conventional plasma proteomic analysis. The elimination of background, highly abundant proteins and the

identification of only the nanoparticle-bound proteins make this nano-platform technology very promising for the discovery of novel diagnostic biomarkers and more studies are needed to explore the prospective applications.

In the present study, we aimed at further exploring the potential use of the proposed nano-scavenger tool in the highly complex clinical challenge of differentiating sepsis from non-infectious acute systemic inflammation in humans. The occurrence of activated systemic inflammation pathways in both conditions adds another level of complexity in comparison to our previous work focusing on the discovery of cancer biomarkers.[18] To prove our hypothesis, we incubated the commercially available amphotericin B-containing liposomes (AmBisome®), clinically used to treat serious, life-threatening fungal infections,[20] with plasma samples obtained from patients with confirmed sepsis and from phenotypically similar sterile tissue injury patients with systemic inflammatory response syndrome (SIRS) (**Figure 1A**). We chose AmBisome® as the preferred liposomal formulation because of its clinical use in high-risk patients with suspected sepsis (most notably in the setting of immunosuppression in hematological oncology, cell and tissue transplantation).[20] Our results demonstrated that comprehensive comparison of the resultant protein coronas led to the identification of 67 potential biomarker proteins that could reproducibly distinguish non-infectious acute systemic inflammation from sepsis.

Results

Physicochemical characterisation of bare and corona-coated Amphotericin B-intercalated liposomes (AmBisome®). Amphotericin B-intercalated liposomes (AmBisome®) were physicochemically and structurally characterised prior to and after their *ex vivo* incubation with human plasma samples obtained from SIRS control group (n=7) and sepsis patients (n=12). Patient clinical characteristics and blood cell culture results are summarized in **Tables S1 and S2**. Liposomes were also incubated with plasma obtained from healthy donors (n=12) as a control. AmBisome® liposomes were allowed to interact with human plasma proteins for 1 hour followed by a two-step purification protocol, for the separation of corona-coated liposomes from unbound and weakly bound plasma proteins, as we have previously described.[18, 19, 21, 22]

Dynamic light scattering (DLS) and negative stain transmission electron microscopy (TEM) were conducted before and after the *ex vivo* incubation of liposomes with human plasma to assess their physicochemical properties prior to and after corona formation (**Figures 1B, S1 and 1C**). The physicochemical characteristics of the commercially available liposomal

formulation AmBisome® employed in this study are summarized in **Figure 1B**. Bare liposomes displayed a mean hydrodynamic diameter of 102.6 nm, a negative surface charge of -54.3 mV and low polydispersity index values (0.093) indicating a narrow size distribution (**Figure 1B**). TEM imaging revealed a well-dispersed liposomal population with a homogenous size distribution correlating that of DLS measurements (**Figure 1C**).

Dynamic light scattering measurements of corona-coated AmBisome® liposomes demonstrated that their size was not significantly affected upon corona formation, while their surface charge was shifted towards less negative values (**Figures 1B and 1S, Table S3**) indicating their interaction with protein molecules. TEM confirmed the presence of protein molecules onto the surface of AmBisome® liposomes and revealed that the recovered corona-coated liposomes remained intact post-incubation with human plasma and purification, showing no structural differences compared to the bare NP (**Figure 1C**).

Quantitative and qualitative comparison of the *ex vivo* protein coronas formed onto AmBisome® liposomes. To quantitatively compare the total amount of protein adhered onto AmBisome® liposomes in the three different conditions under investigation, we calculated the protein binding value (Pb), expressed as the amount of proteins in μg per each μmole of lipid. As shown in **Figure 2A**, the total amount of proteins adsorbed onto liposomes after their incubation with plasma samples obtained from sepsis patients was significantly higher compared to the amount of proteins adsorbed onto liposomes after their incubation with plasma samples obtained from healthy volunteers (** indicates $p<0.01$ ($p=0.0068$) using the non-parametric Kruskal-Wallis test). This clearly indicates that the formation of protein corona onto AmBisome® liposomes is quantitatively influenced by human sepsis condition. This observation is in agreement with our previous studies, showing that the total amount of protein molecules adsorbed onto the NPs surface is determined by the presence or absence of tumorigenesis, reflecting thus the ongoing pathophysiological alterations in blood proteome.[18]

Interestingly, the average Pb values observed post-incubation of AmBisome® liposomes with plasma samples obtained from SIRS patients was similar to that of sepsis patients. This reflects the clinical challenge in differentiating sepsis from other non-infectious events, such as acute trauma and burns. As shown in **Figure 2A**, the SIRS group exhibited greater variations among the individual patients Pb values compared with the healthy controls and the sepsis patients group. This was expected considering that SIRS patients suffered from a wide range of acute inflammation-related pathological conditions other than infection. It is worth mentioning that the total amount of protein adsorbed onto the surface of AmBisome® liposomes was higher

compared to what we have previously observed for PEGylated doxorubicin-encapsulated liposomes (Caelyx®) of similar size.[19] This is in agreement with the literature suggesting that non-PEGylated surfaces tend to adsorb a higher amount of proteins once in contact with biological fluids.[23]

To investigate whether the higher amount of protein adsorbed onto AmBisome® liposomes could offer a comprehensive coverage of the plasma proteome, corona proteins associated with liposomes were separated by SDS-PAGE and visualized by Imperial Protein stain, as illustrated in **Figure 2B**. The elimination of highly abundant proteins allowed the enrichment of the low MW blood proteome, as we have previously reported (**Figure 2B**).[18, 19, 22] Distinct protein bands were profiled in the case of corona samples, while the protein pattern of plasma control verified the masking effect of albumin (**Figure 2B**). In agreement with the BCA assay data, the amount of protein adsorbed onto AmBisome® post-incubation with plasma obtained from sepsis patients was higher in comparison to the total amount adsorbed post-incubation with plasma obtained from healthy volunteers. Similarly, the considerable variation in the total amount of liposome-bound protein (**Figure 2A**) was reflected in the corona profiles of SIRS patients (**Figure 2B**), indicating the high heterogeneity of this group.

The NP protein corona-enabled biomarker discovery to differentiate sepsis from non-infectious acute systemic inflammation. To identify potential biomarker proteins that can differentiate sepsis from non-infectious acute systemic inflammation, we comprehensively characterised and compared the resultant protein coronas by label-free liquid chromatography–mass spectrometry (LC-MS/MS).

Progenesis QI data analysis (version 3.0; Nonlinear Dynamics) enabled us to statistically compare the protein corona profiles of healthy controls, SIRS patients and sepsis patients. Raw data generated from LC-MS/MS analysis were processed and the mean normalized abundance of each group, the relative protein expression (fold-change) and the reliability of measured differences (ANOVA, *p value*) were calculated (**Figure 3, Figure S2 and Tables 1, S4, S5 and S6**). As shown in **Figure S2 and Table S5**, common proteins between the three different groups displayed quantitative differences and enhanced our hypothesis that proteomic analysis of the liposomal protein coronas unravels differences between healthy and diseased states. In order to identify differentially expressed proteins between healthy controls and the sepsis patients, we compared the protein patterns of the *ex vivo* formed coronas. Results were filtered to present a *p value* <0.05 and interestingly, n=135 proteins were found to be differentially expressed, of which

n=88 were upregulated and n=47 were downregulated in sepsis patients samples (**Figure S2B and Table S6**).

Considering that the prevalent challenge in the clinic is to distinguish between sepsis and non-infectious acute systemic inflammation, we performed further analysis focused on the identification of differentially abundant proteins between SIRS controls and sepsis patients. As shown by the normalized abundance values of **Figure 3A and Table S4**, quantitative differences were observed between the two groups with n=67 proteins being differentially expressed (n=34 upregulated; n=33 downregulated), (**Figure 3B, Figure S3 and Table 1**). Interestingly, the clinically-used CRP protein biomarker was not found to be differentially abundant between sepsis patients and SIRS controls (*p value*=0.29, *max fold-change*=1.97, **Table 1 and S4**), which is consistent with its acknowledged lack of diagnostic specificity.[10] We also performed Principal Component Analysis (PCA) to assess whether these 67 identified on the surface of AmBisome® proteins were able to discriminate sepsis from SIRS. Strikingly, PCA analysis unveiled the formation of two distinct clusters (**Figure S3**).

Ingenuity Pathway Analysis (IPA® QIAGEN Bioinformatics) was then performed to investigate if the corona proteins found to be differentially expressed between sepsis and SIRS groups (n=67) have been previously associated with bacterial sepsis and/or infection. Disease and function IPA search revealed the association of n=7 corona proteins with bacterial infection pathways (**Figure 3C and Table S7**): serum amyloid P component (APCS); B-cell lymphoma/leukemia 10 (BCL10), CD5 antigen like (CD5L), gamma-aminobutyric acid type A receptor alpha1 subunit (GABRA1), immunoglobulin heavy constant gamma 3 (IGHG3), immunoglobulin kappa variable 2-24 (IGKV2-24), lipopolysaccharide binding protein (LBP). However, none of the above differentially abundant proteins was previously described in the literature as a potential biomarker for sepsis.

Noteworthy, serum amyloid P has been previously described to act as a pathogen recognition receptor due to its binding affinity towards microbial surface components.[24-26] Another study revealed the key role of APCS in complement-mediated immunity against *Streptococcus pneumoniae*, which suggests that APCS is a significant component of the innate immunity against this pathogen.[27] In addition, B-cell lymphoma/leukemia 10 (BCL10) has been reported to induce the activation of lymphocytes,[28, 29] as well as to be elevated following exposure of intestinal epithelial cells to LPS.[30] Similar to APCS and BCL10, CD5 antigen like (CD5L) has been shown to be implicated in monocyte inflammatory pathways in response to the surface components of bacteria LPS and lipoteichoic acid (LTA).[31] More interestingly, a recent clinical study has shown that CD5L serum levels of 150 sepsis patients were significantly more

elevated on the day of admission to intensive care unit (ICU) than the levels of PCT and CRP compared to ICU controls and healthy controls.[32] As far as lipopolysaccharide binding protein (LBP) concerns, the results has been so far controversial. Some studies have reported a moderate to low diagnostic capacity for sepsis,[33] while others demonstrated that LBP levels were significantly higher in 97% of sepsis patients than healthy controls.[34] The presence of these proteins on the surface of liposomes suggests that the NP-protein corona mirrors the ongoing pathophysiological alterations in plasma.

In order to provide some initial validation of the proteomic data obtained, we performed enzyme-linked immunosorbent assay (ELISA) experiments using plasma samples obtained from the same SIRS and sepsis patient groups. In agreement with our mass spectrometry data, ELISA experiments demonstrated that the amount of the clinically used biomarker CRP, was not significantly different between SIRS and sepsis groups (95% CI, AUC = 0.7619) (**Figure S4**). Interestingly, serum amyloid P (APCS) and cathepsin G (CTSG), identified in the corona samples obtained from SIRS and sepsis patients exhibited higher AUC values than CRP (95% CI, AUC = 0.7937 for APCS and 95% CI, 0=9048 for CTSG).

Overall, we show that the use of a different from our previous studies[18, 19] liposomal formulation, AmBisome®, facilitates the enrichment of complex biofluids with low abundant molecules, enabling thus the discovery of disease-specific biomarkers upon interaction with plasma proteins. The above data suggest that proteomic analysis of the NP coronas uncovers previously unknown potential biomarker proteins that can differentiate sepsis from non-infectious acute systemic inflammation with higher specificity and sensitivity than the clinically used biomarkers.

Discussion

There is an unmet need for the development of biomarkers to rapidly diagnose sepsis and monitor its progression. The complexity of sepsis pathology and the lack of accurate diagnostic tests impede early diagnosis which in turn impact on treatment decision-making.[35] Currently, diagnosis of sepsis relies on the time-consuming process of blood culturing, often associated with false negative results.[4, 5] The diagnostic uncertainty in differentiating patients with sepsis from those suffering from non-infectious acute systemic inflammation makes sepsis the Achilles' heel of health care.[2] The clinically-used diagnostic and disease monitoring blood marker, C reactive protein (CRP) is an indicator of acute-phase responses and thus is unable to distinguish sepsis from other systemic inflammation-associated diseases.[10, 11, 36] In addition, the clinical signs and symptoms of sepsis in its early stages mirror those of non-infectious acute systemic inflammation[12] and this leads to antibiotics being administered to patients with acute sterile inflammation or viral infection. To date, there is no biomarker or any diagnostic test with the capacity to distinguish between sepsis and non-infectious acute systemic inflammation.[37]

Currently available proteomic techniques are capable of sampling a relatively small fraction of the blood proteome which is mainly composed of highly abundant proteins. The signal-to-noise issue, mainly caused by the albumin and immunoglobulins restricts access to the vital diagnostic information that could be obtained.[38-41] _ENREF_36Plasma immunodepletion and fractionation methods are predominantly employed to tackle this issue, however their extensive use leads to a significant loss of the low molecular plasma proteome along with the highly abundant plasma proteins.[39, 42] MS-based proteomics have significantly aided to the discovery of several sepsis biomarkers and provided valuable information about the complex molecular mechanisms underlining this condition.[43] However, to the best of our knowledge, there are only a few proteomic-based studies reporting the discovery of a single biomarker or a panel of biomarkers that can differentiate sepsis from non-infectious acute systemic inflammation.[37, 44]

Even though there is an increasing evidence that nanoparticle-assisted discovery of novel biomarkers by high-throughput proteomics can revolutionise the field of diagnostics,[18, 19] nanoparticles have been so far utilised in the biomarker verification and validation phases to boost immunoassays sensitivities and detect already known biomarker molecules.[45, 46] Specifically in the case of sepsis, NPs have been successfully employed as contrast agents and biosensors[47] to facilitate the detection of either already known protein biomarkers (CRP, PCT),[48] pathogenic DNA[49-52] or bacterial cells[53-56] by amplifying their signal and improving read-outs.

Among the emerging applications, the exploitation of the NP-protein corona for the discovery of novel biomarkers in conjunction with high-throughput proteomics, has been recently proposed by us[17-19] and others.[57, 58] In our previous work, we demonstrated that the spontaneous interaction of intravenously injected clinically-used liposomes with plasma proteins allowed the discovery of multiple proteins differentially abundant between healthy and tumour bearing mice.[18] It should be emphasised that the proposed liposome-based technology facilitates the initial untargeted discovery step of the biomarker development pipeline and not the detection of a specific biomarker molecule for clinical diagnosis.

In this study, we aimed to further explore and validate the use of the human *ex vivo* nanoparticle-protein corona for the discovery of previously undetectable sepsis biomarkers. To evaluate whether the human *ex vivo* protein corona could reveal differences in the complex case of differentiating between two diseased states, we thoroughly characterised and compared the protein corona patterns formed around the clinically-used Amphotericin B-intercalated liposomal formulation (AmBisome®), post-incubation with plasma obtained from healthy donours, SIRS patients and sepsis patients.

Our results here are in agreement with our previous findings in tumour-bearing mice and humans,[18, 19] showing that the protein corona changes both quantitatively (**Figure 2A**) and qualitatively (**Figure 2B and Figure S2**) in the presence or absence of the disease. A significantly higher total amount of protein was adsorbed onto the surface of liposomes after their incubation with plasma from sepsis in comparison with healthy controls (**Figure 2A**). The above differences in the protein corona patterns of healthy individuals compared with sepsis patients reinforce our hypothesis that the NP-protein corona mirrors the ongoing pathophysiological alterations in plasma proteome. Equally consistent with our previous observations[18, 19] were the gel electrophoresis results, demonstrating that the AmBisome® protein corona is reproducibly enriched by low molecular weight proteins (**Figure 2B**), which conventional proteomics are unable to sensitively detect.

Considering that sepsis pathology is a highly complex physiological process, there is a prevalent concord that a panel of multiple biomarkers, rather than a single biomarker will be needed for its accurate diagnosis.[13, 59] The clinically challenging scenario of distinguishing non-infectious acute systemic inflammation from sepsis,[2] prompt us to investigate whether the NP-protein corona platform can be utilised to identify biomarkers specific to sepsis. Comparative analysis between the protein corona fingerprints of SIRS controls and sepsis patients unveiled 67 novel potential biomarkers, with n=34 and n=33 proteins being upregulated and downregulated in sepsis, respectively (**Figures 3A, 3B, S3 and Table 1**). Especially notable was

that the discovered corona proteins presented max fold-change and *p values* much higher than the clinically-used CRP protein biomarker. Indeed, CRP protein was not found to be differentially expressed between SIRS controls and sepsis patients (*p value*>0.05). This observation is consistent with the acknowledged lack of CRP diagnostic specificity[10] and highlights the pressing need for new diagnostic biomarkers. PCA analysis of the 67 identified protein corona biomarkers revealed the formation of two distinct clusters, suggesting that these proteins can differentiate between the two diseased states (**Figure S3**).

To date, there is not any clinically used biomarker that differentiates sepsis from non-infectious acute inflammation. Even though, disease and function IPA search revealed the association of n=7 corona proteins with bacterial infection-related pathways (**Figure 3C**), none of the potential biomarker proteins discovered in this study (n=67) was found to be previously proposed for sepsis diagnosis. This suggests that the NP-corona platform can potentially unravel information about the human pathophysiology and the underlining mechanisms of human bacterial sepsis. ELISA validation experiments demonstrated that the corona proteins APCS and CTSG displayed greater sensitivity and specificity compared to the clinically-used biomarker CRP (**Figure S4**). More work is needed to examine the role of the above-identified proteins in bacterial sepsis and/or inflammation and their potential utility for the development of future diagnostic tests.

In our previous work, we demonstrated that protein crorona analysis formed around Doxil® liposomes enriches the identification of low abundant and low MW proteins allowing an in depth analysis of the plasma proteome. [ref] Here, we explore the exploitation of protein corona or biomarker discovery in a much more clinically challenging scenario. Our results reveal that analysis of protein corona formed around AmBisome® liposomes allows mining of the blood proteome and discovery of potential diagnostic biomarker panels in the presence of severe blood inflammatory responses. AmBisome® liposomes were found to harvest disease-specific molecules upon incubation with plasma, which paves the way towards further development of this technology by using different types of NPs. It is worth mentioning that this study focuses on the initial phase of biomarker discovery, which renders meticulous future exploration on the verification and validation phases of the biomarker development pipeline important, however out of the scope of this work. Clearly, further studies are needed using a higher number of human clinical samples to determine the specificity and sensitivity of the discovered biomarkers that can be used in the future as a meaningful and accurate panel in combination with clinical assessment to diagnose sepsis.

Conclusion

In this study, we describe the formation of protein corona around the clinically-used liposomal Amphotericin B formulation (AmBisome®). Our data reinforces our previous proposition to exploit the nanoparticle-biomolecule corona in order to allow in depth analysis of the blood proteome and to uncover potential biomarker proteins. To explore the adaptability of this nano-scavenging tool to enrich disease-specific molecules with diagnostic potential in a more clinically challenging scenario, we molecularly compared the *ex vivo* coronas formed upon incubation of liposomes with plasma samples obtained from phenotypically identical non-infectious acute systemic inflammation patients and sepsis patients. Despite the similar inflammatory responses arisen in both conditions, proteomic comparison of the biomolecule coronas revealed 67 plasma proteins that could reproducibly differentiate sepsis from non-infectious acute systemic inflammation. The nanoparticle-corona platform has the potential to accelerate the development of panels of biomarkers that can in combination with clinical evaluation rapidly and accurately diagnose sepsis, limiting unnecessary antibiotic treatments.

Experimental

Ethical approvals of patient plasma samples. The patient samples were collected and stored at Salford Royal NHS Foundation Trust following review and approval by the NHS National Research Ethics Service Committee North West – Greater Manchester South (Ref#14/NW/1404). Sample collection from patients was undertaken by designated members from Salford Royal NHS Foundation Trust's research and development team. All experiments were performed in compliance with the University of Manchester policy on human plasma use and ethics.

Selection of patient samples. Suitable patient samples were identified via study case report forms. The selection of patient samples was based on the clinical criteria for acute systemic inflammation and the blood/urine culture results. For inclusion in the sepsis group, patients had to have blood culture evidence of bacterial infection and a score of 2 or more out of 4 criteria for acute systemic inflammation.[1] For patients to be included in the non-infectious acute systemic inflammation group, they had to have 2 or more clinical criteria for acute systemic inflammation, no clinical or microbiological laboratory evidence of infection (negative blood/urine culture tests) and given no more than one dose of antibiotics.

Blood samples collection. Blood samples from patients had been collected after recognition of a score of two or more (out of 4) clinical criteria for acute systemic inflammation, and immediately prior to antibiotic administration. Samples were collected in commercially available anticoagulant-treated tubes (K2 EDTA BD Vacutainer®). Plasma was then prepared by inverting the collection tubes to ensure mixing of blood with EDTA and subsequent centrifugation for 15 minutes at 1500x g at 4 ^{0}C. Following centrifugation, supernatant was immediately collected into labelled 1.5 mL screw-cap polypropylene tubes (Thermo Fisher), and samples were maintained on dry ice while handling. Finally, samples were stored in a -80 ^{0}C freezer and were thawed only before the incubations.
For the *ex vivo* protein binding study of healthy controls, 6 female and 6 male human samples were supplied by Seralab, UK, Batches #BRH1401254 (H1), #BRH1401253 (H2), #BRH1401256 (H3), #BRH1401259 (H4), #BRH1401252 (H5), #BRH1401257 (H6), #BRH1401243 (H7), #BRH1401247 (H8), #BRH1401244 (H9), #BRH1401246 (H10), #BRH1401249 (H11) and #BRH1401248 (H12). Considering the impact of the anticoagulant agent on the formation of the protein corona,[60] healthy plasma samples contained the same anticoagulant agent (K2 EDTA BD Vacutainer® tubes) as that described above for the human clinical samples and were subjected to the same preparation protocol (centrifugation for 12 min at 1300 rpm at 4 ^{0}C). Healthy human plasma samples were received on dry ice and were stored in a -80 ^{0}C freezer upon arrival from Seralab, UK. Finally, samples were thawed only before the incubations.

Preparation of AmBisome® liposomes suspension. 2 vials of AmBisome® liposomal formulation (HSPC:Cholesterol:DSPG:Amphotericin B, batch #006572D) were kindly donated by Salford Royal NHS Foundation Trust's research and development team. 12 mL of HEPES buffer solution (HBS, 150 mM NaCl (Sigma Aldrich, S6191) and 20 mM HEPES (Sigma Aldrich, H3375), pH=7.4) were added to the vial and the reconstituted suspension was gently and thoroughly mixed. The concentration of liposomes in the reconstituted suspension was quantified by Stewart assay (see below) and was found to be ~41 mM.

***Ex vivo* incubation of AmBisome® liposomes with human plasma.** The *ex vivo* protein corona was allowed to form using AmBisome® liposomal formulation. AmBisome® was added into human plasma obtained from healthy individuals (n=12), non-infectious acute systemic inflammation (SIRS) patients (n=7) and sepsis patients (n=12). A concentration of 1 mM of liposomes (1 mM lipids/mL blood) was chosen for incubation based upon a dose of 3 mg of Amphotericin B/kg body weight.[61, 62] Thus, 24 µL of AmBisome® were incubated with 820 µL of human plasma and 156 µL of HEPES buffer solution (HBS) to reach 1 mL volume for 1 hour at 37 ^{0}C in orbital shaker (ThermoFisher, MaxQ™ 4450 Benchtop Orbital Shaker) at 250 rpm, set to mimic *in vivo* conditions. 1 hour of *ex vivo* incubation was chosen because it is the equivalent time for the infusion of AmBisome®.

Separation of corona-coated AmBisome® liposomes from unbound and weakly bound proteins. Corona-coated liposomes were separated form excess plasma proteins following a two-step purification protocol, including size exclusion chromatography and membrane ultrafiltration, as we have previously described.[18, 19, 21, 22]

Size and zeta potential measurements using dynamic light scattering (DLS). The size and surface charge of AmBisome® liposomes were measured by Intensity using a Zetasizer Nano ZS (Malvern, Instruments, UK). For both size and ζ-potential measurements, samples were diluted with ultra-pure water in 1 mL polystyrene disposable cuvettes and 1 mL disposable Zetasizer cuvettes, respectively. Size and ζ-potential data was taken in three records.

Transmission Electron Microscopy (TEM). Liposomes were visualized with transmission electron microscopy (FEI Tecnai 12 BioTwin) before and after their *ex vivo* interaction with human plasma proteins. 10 uL of each sample were diluted in 600 uL of ultra-pure water. A drop from each sample was placed onto a Carbon Film Mesh Copper Grid (CF400-Cu, Electron Microscopy Science) and subsequently was stained using aqueous uranyl acetate solution 1%.

SDS-PAGE electrophoresis. Proteins associated with 0.025 μM of liposomes were loaded in 4-20% Novex™ Tris-Glycine Protein Gels (WedgeWell™, ThermoFisher Scientific) along with a 10 – 180 kDa Prestained Protein Ladder (PageRuler™ Prestained Protein Ladder 10 – 180 kDa, ThermoFisher Scientific) and run through a 10 times diluted 10xNovex™ Tris-Glycine SDS Running Buffer (ThermoFisher Scientific) in ultra-pure water for 25-40 minutes at 225 V and 125 mA until the proteins reached the end of the gel. Gels were stained for 1 hour using the Imperial protein Gel Staining reagent (Imperial protein stain, ThermoFisher Scientific) followed by a couple of washings with ultra-pure water for 1-2 days.

Quantification of recovered lipids and adsorbed proteins. Lipid concentration (mM) was quantified by Stewart Assay using a Cary 50 Bio Spectrophotometer (Agilent Technologies), as we have previously described.[18, 19, 21, 22] The total amount of the adsorbed proteins onto the surface of AmBisome® was quantified by BCA Protein assay kit (ThermoFisher Scientific), according to the manufacturer's instructions, using a plate reader (Fluostar Omega plate reader, BMG Labtech). Protein binding (Pb) values, expressed as μg of protein/μmole of lipid were then calculated per patient and per group, presented as the average ± standard deviation (healthy controls n=12, SIRS patients n=7 and sepsis patients n=12).

Mass Spectrometry. Corona proteins (20 μg) were loaded in 10 % NOVEX Tris-Glycine Protein Gels (WedgeWell™, ThermoFisher Scientific) and run through a 10 times diluted 10xNovex® Tris-Glycine SDS Running Buffer (ThermoFisher Scientific) in ultra-pure water for 2-5 minutes at 225 V and 125 mA until the formation of a single band at the top of the gel. Gels were stained for 1 hour using the Imperial protein Gel Staining reagent (Sigma Life Science) followed by a couple of washings with ultra-pure water for 1-2 days. Gel bands were cut out in 1 mm small square pieces and placed into 96 perforated plate wells. Samples were reduced with 10 mM dithiothreitol, alkylated with 55 mM iodoacetamide, washed with ammonium bicarbonate and acetonitrile and digested by 12.5 ng/μL trypsin overnight at 37 ^{0}C. Following overnight incubation, samples were extracted using 20 mM ammonium bicarbonate and 50 % acetonitrile, 5 % formic acid, desalted and dried by vacuum centrifugation. Dried samples were reconstituted in 10 μL 5 % acetonitrile 0.1 % formic acid and analyzed by LC-MS/MS using an UltiMate® 3000 Rapid Separation LC (RSLC, Dionex Corporation, Sunnyvale, CA) coupled to a Q Exactive™ Hybrid Quadrupole-Orbitrap™ (ThermoFisher Scientific, Waltham, MA) mass spectrometer.

Mass Spectrometry Data Analysis. RAW files were imported into Progenesis LC-MS software (version 3.0; Nonlinear Dynamics) with automatic feature detection enabled. A representative reference run was selected automatically to which all other runs were aligned in a pair-wise manner. Automatic processing was selected to run with applied filters for peaks charge state (maximum charge 5) and protein quantitation method the relative quantitation using Hi-N with N=3 peptides to measure per protein. The resulting MS/MS peak lists were exported as a single Mascot generic file and loaded onto a local Mascot Server (Matrix Science, London, UK; version 2.5.1). The spectra were searched against the SwissProt_2018_01 database (selected for *Homo sapiens*, 161629 entries) using the following parameters: tryptic enzyme digestion with one missed cleavage allowed, peptide charge of +2 and +3, precursor mass tolerance of 15 mmu, fragment mass tolerance of 8 ppm, oxidation of methionines as variable modifications and carbamidomethyl as fixed modifications, with decoy database search disabled

and ESI-QUAD-TOF the selected instrument. Each search produced an XML file from Mascot and the resulted peptides (XML files) were imported back into Progenesis LC-MS to assign peptides to features. Data was filtered to present a score above 21 through the 'refine identification' tab of Progenesis QI toolbox. A table of all identified features along with their normalized peptide and protein abundance in each sample was generated. The max fold-change and p value (ANOVA) of each protein was then calculated by Progenesis and data including the normalized abundance, p-value and max fold-change were exported for further analysis. Finally, results were filtered to present a mean normalized abundance of more than 50,000 in at least one of the three groups.
Mass Spectrometry data was further analyzed through the use of QIAGEN's Ingenuity Pathway Analysis® (IPA®, QIAGEN Redwood City, www.qiagen.com/ingenuity). Diseases and functions IPA tool was used to identify proteins involved in inflammation and bacterial infection pathways. The biomarker overlay IPA tool was then used to identify proteins described in the literature as potential systemic inflammatory response and sepsis biomarkers for diagnosis, efficacy or any unspecified application.

Enzyme-linked Immunosorbent Assay (ELISA). Sandwich-ELISA kits for the human proteins CRP (CRP, ab99995, Abcam, UK), serum amyloid P (APCS, ab137970, Abcam, UK) and cathepsin G (CTSG, abx251221, Abbexa Ltd, UK) were purchased for the quantitative measurement of each corona protein in plasma. Experiments were performed according to manufacturer's instructions. All assays employed an antibody specific for each human protein coated on a 96-well plate. Standards and samples were pipetted into the wells and protein present in a sample was bound to the wells by the immobilized antibody. The wells were then washed and biotinylated anti-human protein antibody was added. After washing away unbound biotinylated antibody, HRP-conjugated Streptavidin was pipetted to the wells. Following a second washing, a TMB substrate solution was added to each well to allow colour development in proportion to the amount of each bound protein. Finally, stop solution was added to the wells, colour changed from blue to yellow and the absorbance was measured at 450 nm using a plate reader (Fluostar Omega plate reader, BMG Labtech). A standard curve was prepared based upon the intensity of the colour of the standard solutions by GraphPad Prism 7 regression analysis and the concentration of the bound protein per sample was calculated.

Statistical analysis. Statistical analysis of the data was performed using GraphPad Prism 7 software. The non-parametric Kruskal-Wallis tests was used and p values<0.05 were considered significant. Receiver operating curves (ROC) and the respective Area under the Curve (AUC) values were produced and calculated based on the ELISA data of each selected for validation protein using GraphPad Prism 7 software (**Figure S3**).

Conflicts of interest

There are no conflicts to declare.

Author contributions

L.P., A.C. and M.H. designed and performed the experiments, analyzed all data and took responsibility for planning and writing the manuscript. A.C. and P.D. contributed to the clinical design, provided oversight of the ethical approval process and were responsible for access and storage of the samples in the Salford Royal NHS Foundation Trust. P.D., M.H. and K.K. initiated, designed, directed, provided intellectual input throughout the study and contributed to the writing of the manuscript.

Acknowledgements

This research was partially funded by the Manchester Molecular Pathology Innovation Centre (MMPathIC). Authors wish to acknowledge Salford Royal NHS Foundation Trust's research and development team for their assistance in the collection of blood samples. The authors also wish to thank the Faculty of Life Sciences EM Facility at the University of Manchester for their assistance in Electron Microscopy imaging. In addition, Mass Spectrometry Facility staff at the University of Manchester for their support. We would also like to thank the patients for their kind donation of blood samples to support this research.

FIGURE LEGENDS

Figure 1: Physicochemical characterization of corona-coated Amphotericin B-intercalated liposomes (AmBisome®). (A) Schematic description of the experimental design. Liposomes were incubated *ex vivo* (1 hour at 37^0C, 250 rpm) with human plasma samples obtained from a) healthy donors (n=12), b) SIRS patients (n=7) and c) sepsis patients (n=12). *Ex vivo* corona-coated liposomes were recovered and purified from unbound proteins and the formed protein coronas were qualitatively and quantitatively characterised and compared between the groups; **(B)** Mean hydrodynamic diameter (nm) and ζ-potential (mV) distributions for the liposomal formulation AmBisome®, before and after *ex vivo* incubation with human plasma. Table shows the average mean hydrodynamic diameter (nm), polydispersity index (PDI) and ζ-potential (mV) values of bare and corona-coated liposomes; **(C)** Negative stain TEM imaging of bare and corona-coated AmBisome® liposomes, recovered post-incubation with human plasma obtained from healthy controls, SIRS patients and sepsis patients. All scale bars are 100 nm.

Figure 2: Quantitative and qualitative comparison of the *ex vivo* protein coronas formed onto AmBisome® liposomes. **(A)** Comparison of the total amount of protein adsorbed onto liposomes after their *ex vivo* incubation with plasma obtained from healthy donors (n=12), SIRS patients (n=7) and sepsis patients (n=12), (expressed as μg protein/μmole of NP). Pb values represent the average and standard error. ** indicates $p<0.01$ ($p=0.0068$) between healthy donors and sepsis patients using the non-parametric Kruskal-Wallis test; **(B)** Imperial stained SDS-PAGE gels of plasma control and corona proteins associated with liposomes after incubation with plasma obtained from healthy donors, SIRS patients and sepsis patients.

Figure 3: The NP protein corona-enabled biomarker discovery to differentiate sepsis from non-infectious acute systemic inflammation. (A) Heatmap of normalized abundance values of corona proteins differentially abundant between SIRS controls and sepsis patients, after identification by LC-MS/MS and data analysis by Progenesis QI. Protein columns are sorted according to the abundance values (from highest to lowest) of the first sample. The list of proteins shown in the heatmap and their respective accession numbers, p-values and max fold-change are shown in **Table S4**; **(B)** Volcano plot represents the potential protein biomarkers differentially abundant between sepsis group and SIRS control group (n=67) identified in corona samples. Upregulated biomarkers in sepsis group are shown in red (n=34), whereas downregulated biomarkers in the presence of sepsis are shown in blue colour (n=33). Only proteins with p value<0.05 are reported. The list of proteins shown in the volcano plot and their respective accession numbers, p-values and max fold-change are shown in **Table 1**; **(C)** Ingenuity Pathway Analysis (IPA) of potential biomarker corona proteins associated with bacterial infection. The name of proteins illustrated in the diagram and their respective gene symbol are shown in **Table S7**.

FIGURE 1

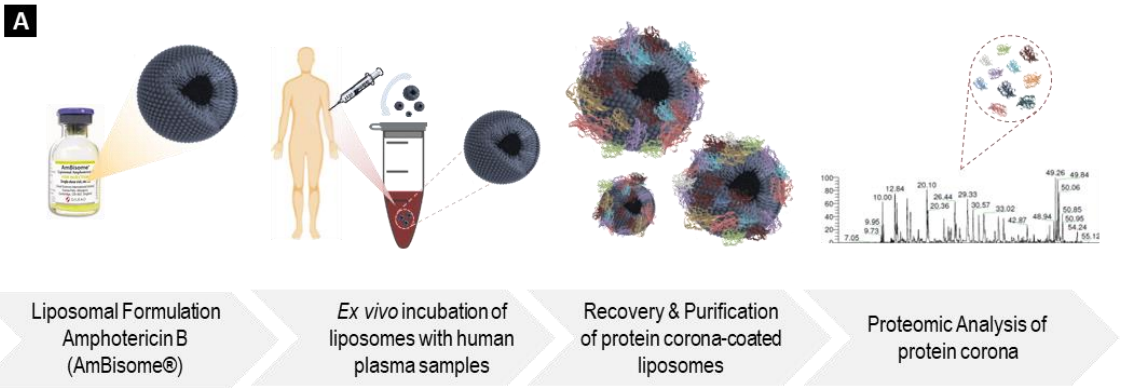

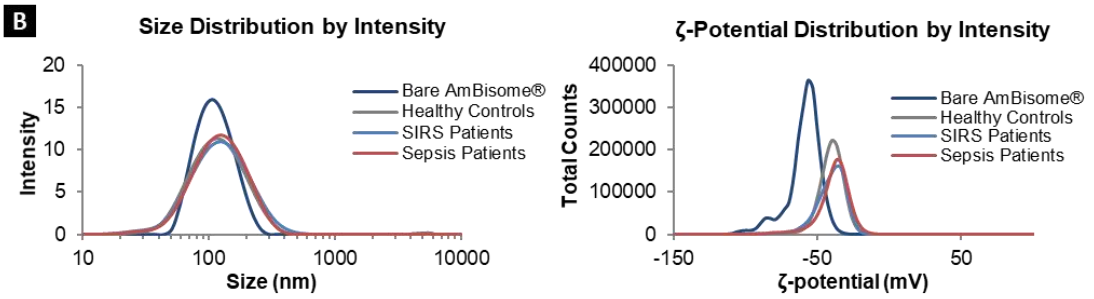

Sample Name	Mean Hydrodynamic Diameter (nm)	PDI	ζ-potential (mV)
Bare AmBisome®	102.6 ± 1.7	0.093 ± 0.016	-54.3 ± 4.3
Healthy Controls	104.4 ± 7.8	0.224 ± 0.028	-40.4 ± 2.4
SIRS Patients	106.5 ± 5.5	0.217 ± 0.049	-38.7 ± 5.7
Sepsis Patients	106.4 ± 8.9	0.199 ± 0.026	-38.5 ± 2.9

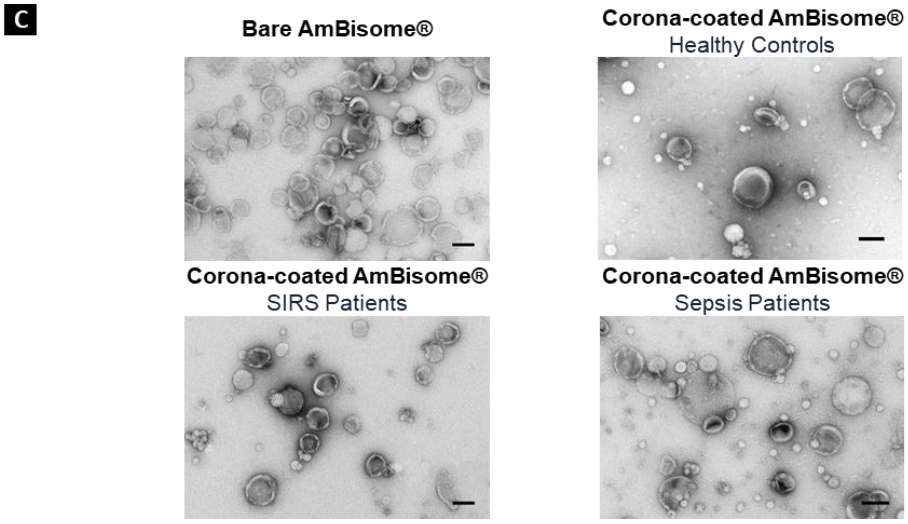

FIGURE 2

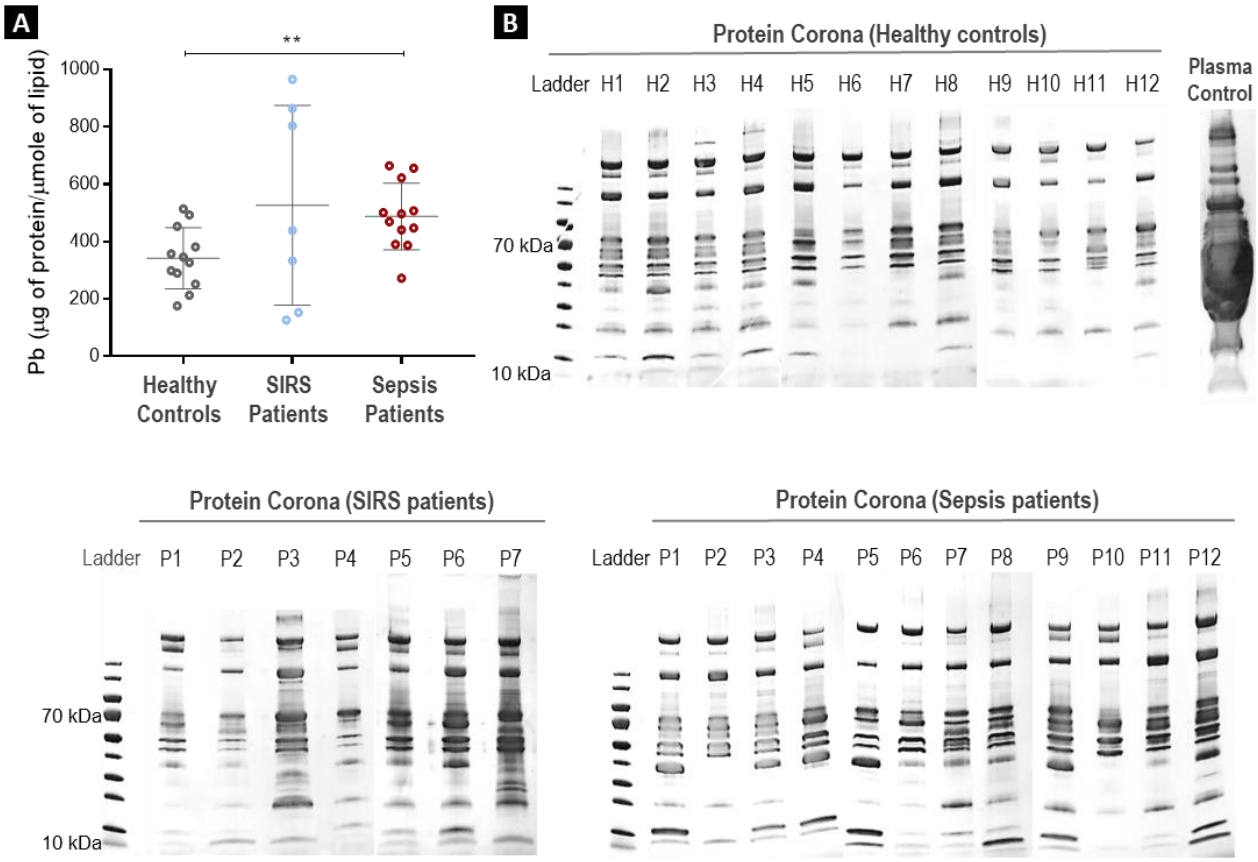
A
**
Pb (µg of protein/µmole of lipid)
1000
800
600
400
200
0
Healthy Controls
SIRS Patients
Sepsis Patients
B
Protein Corona (Healthy controls)
Ladder H1 H2 H3 H4 H5 H6 H7 H8 H9 H10 H11 H12
Plasma Control
70 kDa
10 kDa
Protein Corona (SIRS patients)
Ladder P1 P2 P3 P4 P5 P6 P7
70 kDa
10 kDa
Protein Corona (Sepsis patients)
Ladder P1 P2 P3 P4 P5 P6 P7 P8 P9 P10 P11 P12

FIGURE 3

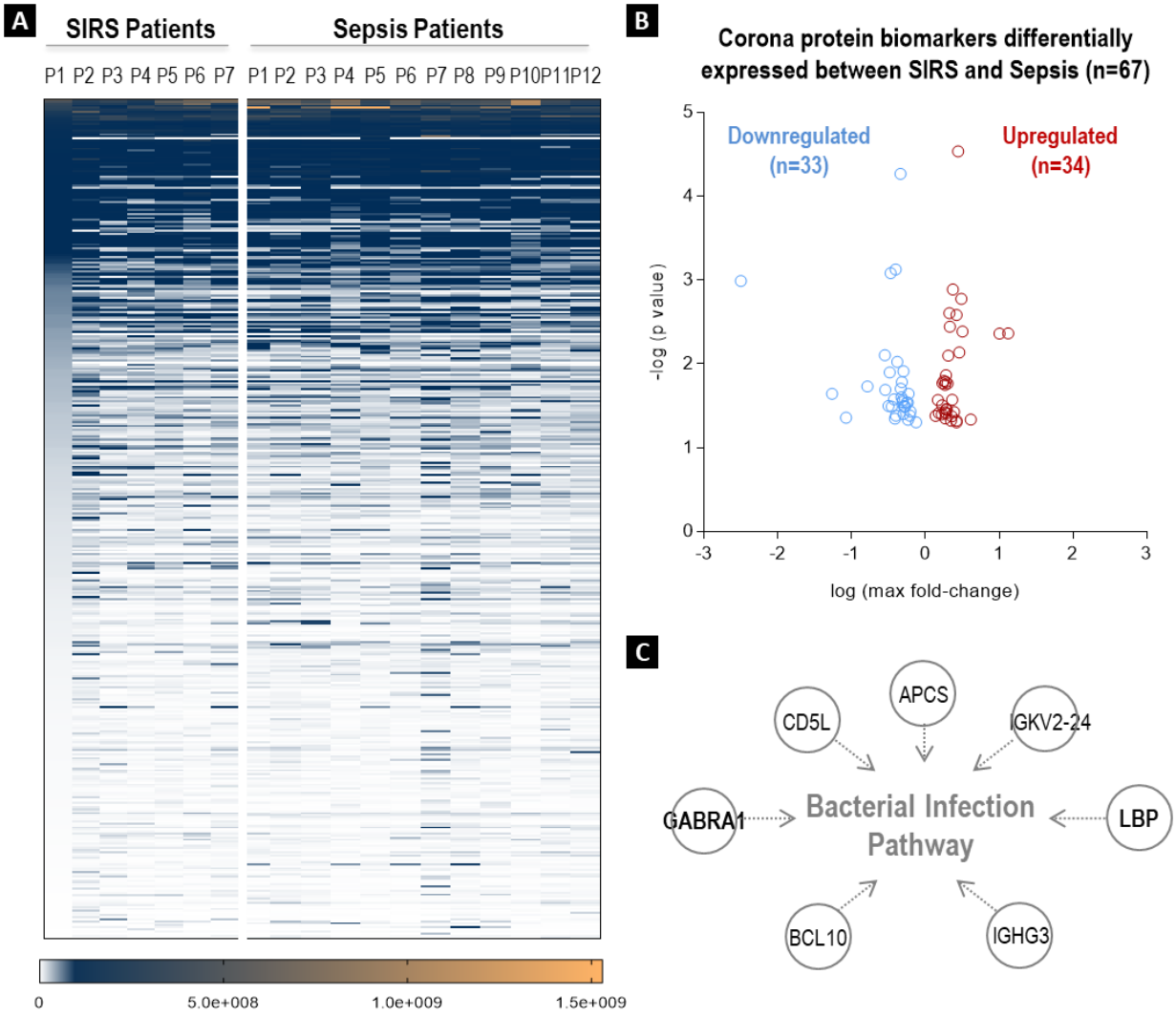
A
SIRS Patients
Sepsis Patients
P1 P2 P3 P4 P5 P6 P7 P1 P2 P3 P4 P5 P6 P7 P8 P9 P10P11P12
0
5.0e+008
1.0e+009
1.5e+009
B
Corona protein biomarkers differentially expressed between SIRS and Sepsis (n=67)
Downregulated (n=33)
Upregulated (n=34)
-log (p value)
log (max fold-change)
C
CD5L
APCS
IGKV2-24
GABRA1
Bacterial Infection Pathway
LBP
BCL10
IGHG3

TABLE 1

Table 1: Candidate corona protein biomarkers for differentiating between sepsis and non-infectious acute systemic inflammation patients, as identified by proteomic analysis of the *ex vivo* liposome coronas. Full list of proteins identified by Progenesis QI for proteomics to be upregulated or downregulated in sepsis patients in comparison with SIRS controls classified from the highest max fold-change to the lowest. Only proteins with $p<0.05$ are shown.

Identified Proteins (n=67)	Accession Number	Anova (p)	Max fold change
UPREGULATED			
OTU domain-containing protein 7A	OTU7A_HUMAN	4.32E-03	13.23
Immunoglobulin kappa variable 1D-13	KVD13_HUMAN	4.34E-03	10.14
Dual specificity mitogen-activated protein kinase kinase 7	MP2K7_HUMAN	4.60E-02	4.11
NEDD4-binding protein 2	N4BP2_HUMAN	4.11E-03	3.19
Complement component C8 gamma chain	CO8G_HUMAN	1.68E-03	3.07
Sentrin-specific protease 2	SENP2_HUMAN	7.28E-03	2.88
Ficolin-2	FCN2_HUMAN	2.92E-05	2.79
Fibulin-1	FBLN1_HUMAN	2.62E-03	2.64
Endophilin-A3	SH3G3_HUMAN	4.97E-02	2.64
Sorting nexin-32	SNX32_HUMAN	4.75E-02	2.64
Immunoglobulin heavy constant gamma 2	IGHG2_HUMAN	3.75E-02	2.44
Complement component C7	CO7_HUMAN	1.29E-03	2.36
Immunoglobulin gamma-1 heavy chain	IGG1_HUMAN	2.69E-02	2.31
Immunoglobulin heavy constant gamma 3	IGHG3_HUMAN	4.21E-02	2.28
Unconventional myosin-XV	MYO15_HUMAN	4.77E-02	2.22
Inter-alpha-trypsin inhibitor heavy chain H4	ITIH4_HUMAN	3.59E-03	2.14
Complement C5	CO5_HUMAN	2.49E-03	2.12
Hemoglobin subunit alpha	HBA_HUMAN	7.97E-03	2.04
Complement component C6	CO6_HUMAN	1.72E-02	2.00
Complement component C8 beta chain	CO8B_HUMAN	3.47E-02	1.94
Synapsin-3	SYN3_HUMAN	3.89E-02	1.91
Hemoglobin subunit delta	HBD_HUMAN	1.36E-02	1.90
Inter-alpha-trypsin inhibitor heavy chain H3	ITIH3_HUMAN	3.51E-02	1.90
Complement factor H-related protein 1	FHR1_HUMAN	1.64E-02	1.89
Lipopolysaccharide-binding protein	LBP_HUMAN	4.48E-02	1.86
FANCD2 opposite strand protein	FACOS_HUMAN	3.76E-02	1.85
Complement C3	CO3_HUMAN	1.77E-02	1.85
Fibrinogen alpha chain	FIBA_HUMAN	1.59E-02	1.78
Histone H2B type 1-A	H2B1A_HUMAN	1.70E-02	1.70
Serum amyloid P-component	SAMP_HUMAN	3.12E-02	1.68
Carboxypeptidase N catalytic chain	CBPN_HUMAN	3.98E-02	1.66
Complement factor H	CFAH_HUMAN	3.87E-02	1.53
Hemoglobin subunit beta	HBB_HUMAN	2.69E-02	1.48
Vitronectin	VTNC_HUMAN	4.17E-02	1.38

Identified Proteins (n=67)	Accession Number	Anova (p)	Max fold change
DOWNREGULATED			
N-terminal EF-hand calcium-binding protein 2	NECA2_HUMAN	1.02E-03	317.68
Flotillin-2	FLOT2_HUMAN	2.27E-02	18.41
Dematin	DEMA_HUMAN	4.38E-02	11.90
B-cell lymphoma/leukemia 10	BCL10_HUMAN	1.86E-02	6.11
ATP-dependent 6-phosphofructokinase, liver type	PFKAL_HUMAN	7.88E-03	3.56
Cancer-associated gene 1 protein	CAGE1_HUMAN	2.04E-02	3.51
Ras-related protein Ral-B	RALB_HUMAN	3.18E-02	3.17
Immunoglobulin lambda variable 1-44	LV144_HUMAN	1.26E-02	3.05
Guanine nucleotide-binding protein G(i) subunit alpha-2	GNAI2_HUMAN	8.28E-04	2.96
Cytoplasmic dynein 1 heavy chain 1	DYHC1_HUMAN	3.24E-02	2.86
Immunoglobulin kappa variable 1-12	KV112_HUMAN	2.64E-02	2.65
Aminopeptidase N	AMPN_HUMAN	4.48E-02	2.59
Tenascin-X	TENX_HUMAN	7.46E-04	2.54
Immunoglobulin heavy variable 3-48	HV348_HUMAN	4.13E-02	2.51
Immunoglobulin kappa variable 1-17	KV117_HUMAN	9.46E-03	2.40
Ubiquitin-40S ribosomal protein S27a	RS27A_HUMAN	5.41E-05	2.17
Gamma-aminobutyric acid receptor subunit alpha-1	GBRA1_HUMAN	1.98E-02	2.16
Serine/arginine-rich splicing factor 4	SRSF4_HUMAN	2.50E-02	2.11
Immunoglobulin heavy variable 6-1	HV601_HUMAN	1.65E-02	2.08
Annexin A2	ANXA2_HUMAN	2.84E-02	2.04
Sulfhydryl oxidase 2	QSOX2_HUMAN	2.70E-02	2.03
PI-PLC X domain-containing protein 2	PLCX2_HUMAN	1.23E-02	1.99
Immunoglobulin kappa variable 1-5	KV105_HUMAN	3.97E-02	1.99
Immunoglobulin heavy variable 3-23	HV323_HUMAN	3.20E-02	1.96
Immunoglobulin kappa variable 2-24	KV224_HUMAN	3.17E-02	1.90
Immunoglobulin lambda variable 2-11	LV211_HUMAN	3.28E-02	1.90
Desmoglein-1	DSG1_HUMAN	2.90E-02	1.79
Immunoglobulin lambda variable 1-51	LV151_HUMAN	2.88E-02	1.73
CD5 antigen-like	CD5L_HUMAN	4.63E-02	1.72
Immunoglobulin kappa variable 3-11	KV311_HUMAN	2.28E-02	1.69
Apolipoprotein L1	APOL1_HUMAN	4.15E-02	1.62
Oxysterol-binding protein-related protein 11	OSB11_HUMAN	3.70E-02	1.60
Vitamin K-dependent protein S	PROS_HUMAN	4.96E-02	1.34

References

1. M. Singer, C. S. Deutschman, C. W. Seymour, M. Shankar-Hari, D. Annane, M. Bauer, et al., *JAMA*, 2016, **315**, 801-810.
2. K. Reinhart, R. Daniels, N. Kissoon, F. R. Machado, R. D. Schachter and S. Finfer, *New England Journal of Medicine*, 2017, **377**, 414-417.
3. R. Ferrer, I. Martin-Loeches, G. Phillips, T. M. Osborn, S. Townsend, R. P. Dellinger, et al., *Critical Care Medicine*, 2014, **42**, 1749-1755.
4. K. Chun, C. Syndergaard, C. Damas, R. Trubey, A. Mukindaraj, S. Qian, et al., *J Lab Autom*, 2015, **20**, 539-561.
5. J. Phua, W. Ngerng, K. See, C. Tay, T. Kiong, H. Lim, et al., *Crit Care*, 2013, **17**, R202.
6. A. Rhodes, L. E. Evans, W. Alhazzani, M. M. Levy, M. Antonelli, R. Ferrer, et al., *Intensive Care Medicine*, 2017, **43**, 304-377.
7. C. A. Michael, D. Dominey-Howes and M. Labbate, *Front Public Health*, 2014, **2**, 145.
8. J. D. Faix, *Crit Rev Clin Lab Sci*, 2013, **50**, 23-36.
9. K. R. Walley, *Curr Infect Dis Rep*, 2013, **15**, 413-420.
10. B. Clyne and J. S. Olshaker, *J Emerg Med*, 1999, **17**, 1019-1025.
11. B. M. Tang, G. D. Eslick, J. C. Craig and A. S. McLean, *Lancet Infect Dis*, 2007, **7**, 210-217.
12. J. L. Vincent, *PLoS Med*, 2016, **13**, e1002022.
13. V. Sankar and N. R. Webster, *J Anesth*, 2013, **27**, 269-283.
14. N. L. Anderson and N. G. Anderson, *Molecular & Cellular Proteomics*, 2003, **2**, 50-50.
15. K. Hamad-Schifferli, *Nanomedicine (Lond)*, 2015, **10**, 1663-1674.
16. T. Cedervall, I. Lynch, S. Lindman, T. Berggard, E. Thulin, H. Nilsson, et al., *Proc Natl Acad Sci U S A*, 2007, **104**, 2050-2055.
17. M. Hadjidemetriou and K. Kostarelos, *Nature Nanotechnology*, 2017, **12**, 288-290.
18. M. Hadjidemetriou, Z. Al-Ahmady, M. Buggio, J. Swift and K. Kostarelos, *Biomaterials*, 2018, **188**, 118-129.
19. M. Hadjidemetriou, S. McAdam, G. Garner, C. Thackeray, D. Knight, D. Smith, et al., *Adv Mater*, 2018, DOI: 10.1002/adma.201803335, e1803335.
20. M. D. Moen, K. A. Lyseng-Williamson and L. J. Scott, *Drugs*, 2009, **69**, 361-392.
21. M. Hadjidemetriou, Z. Al-Ahmady, M. Mazza, R. F. Collins, K. Dawson and K. Kostarelos, *ACS Nano*, 2015, **9**, 8142-8156.
22. M. Hadjidemetriou, Z. Al-Ahmady and K. Kostarelos, *Nanoscale*, 2016, **8**, 6948-6957.
23. Q. Dai, C. Walkey and W. C. Chan, *Angew Chem Int Ed Engl*, 2014, **53**, 5093-5096.
24. C. J. C. de Haas, M. E. van der Tol, K. P. M. Van Kessel, J. Verhoef and J. A. G. Van Strijp, *J Immunol*, 1998, **161**, 3607-3615.
25. C. J. C. de Haas, *Fems Immunol Med Mic*, 1999, **26**, 197-202.
26. R. A. Schwalbe, B. Dahlback, J. E. Coe and G. L. Nelsestuen, *Biochemistry-Us*, 1992, **31**, 4907-4915.
27. J. Yuste, M. Botto, S. E. Bottoms and J. S. Brown, *Plos Pathog*, 2007, **3**, 1208-1219.
28. S. W. Li, X. Yang, J. Shao and Y. Q. Shen, *Plos One*, 2012, **7**.
29. H. Y. Lu, B. M. Bauman, S. Arjunaraja, B. Dorjbal, J. D. Milner, A. L. Snow, et al., *Front Immunol*, 2018, **9**.
30. S. Bhattacharyya, A. Borthakur, N. Pant, P. K. Dudeja and J. K. Tobacman, *Am J Physiol Gastrointest Liver Physiol*, 2007, **293**, G429-437.
31. L. Sanjurjo, N. Amezaga, G. Aran, M. Naranjo-Gomez, L. Arias, C. Armengol, et al., *Autophagy*, 2015, **11**, 487-502.
32. X. Gao, Y. Liu, F. Xu, S. Lin, Z. Song, J. Duan, et al., *Chest*, 2019, DOI: 10.1016/j.chest.2019.04.134.

33. K. F. Chen, C. H. Chaou, J. Y. Jiang, H. W. Yu, Y. H. Meng, W. C. Tang, et al., *Plos One*, 2016, **11**, e0153188.
34. S. M. Opal, P. J. Scannon, J. L. Vincent, M. White, S. F. Carroll, J. E. Palardy, et al., *J Infect Dis*, 1999, **180**, 1584-1589.
35. R. S. Hotchkiss, L. L. Moldawer, S. M. Opal, K. Reinhart, I. R. Turnbull and J. L. Vincent, *Nat Rev Dis Primers*, 2016, **2**, 16045.
36. C. Pierrakos and J.-L. Vincent, *Critical Care* 2010, **14**.
37. T. C. Hall, D. K. Bilku, D. Al-Leswas, C. Horst and A. R. Dennison, *Ir J Med Sci*, 2011, **180**, 793-798.
38. K. Merrell, K. Southwick, S. W. Graves, M. S. Esplin, N. E. Lewis and C. D. Thulin, *J Biomol Tech*, 2004, **15**, 238-248.
39. C. E. Parker and C. H. Borchers, *Mol Oncol*, 2014, **8**, 840-858.
40. L. A. Liotta, M. Ferrari and E. Petricoin, *Nature*, 2003, **425**, 905.
41. R. Schiess, B. Wollscheid and R. Aebersold, *Mol Oncol*, 2009, **3**, 33-44.
42. N. Rifai, M. A. Gillette and S. A. Carr, *Nature Biotechnology*, 2006, **24**, 971-983.
43. Z. Cao and R. A. Robinson, *Proteomics Clin Appl*, 2014, **8**, 35-52.
44. M. E. Lissauer, S. B. Johnson, G. Siuzdak, G. Bochicchio, C. Whiteford, B. Nussbaumer, et al., *J Trauma*, 2007, **62**, 1082-1092; discussion 1092-1084.
45. J. Kim, M. A. Abdou Mohamed, K. Zagorovsky and W. C. W. Chan, *Biomaterials*, 2017, **146**, 97-114.
46. X. Zhu, A. F. Radovic-Moreno, J. Wu, R. Langer and J. Shi, *Nano Today*, 2014, 478-498.
47. P. D. Howes, R. Chandrawati and M. M. Stevens, *Science*, 2014, **346**, 1247390.
48. A. H. Nguyen, Y. Shin and S. J. Sim, *Biosensors and Bioelectronics*, 2016, **85**, 522-528.
49. H. J. Chung, C. M. Castro, H. Im, H. Lee and R. Weissleder, *Nature Nanotechnology*, 2013, **8**, 369-375.
50. M. Liong, A. N. Hoang, J. Chung, N. Gural, C. B. Ford, C. Min, et al., *Nat Commun*, 2013, **4**, 1752.
51. J. J. Storhoff, A. D. Lucas, V. Garimella, P. Y. Bao and U. R. Mueller, *Nature Biotechnology*, 2004, **22**, 883-887.
52. H. D. Hill and C. A. Mirkin, *Nature Protocols*, 2006, **1**, 324-336.
53. B. A. Borsa, B. G. Tuna, F. J. Hernandez, L. I. Hernandez, G. Bayramoglu, M. Y. Arica, et al., *Biosensors and Bioelectronics*, 2016, **86**, 27-32.
54. D. Issadore, H. J. Chung, J. Chung, C. Budin, R. Weissleder and H. Lee, *Advanced Healthcare Materials*, 2013, 1224-1228.
55. C.-I. Weng, H.-T. Chang, C.-H. Lin, Y.-W. Shen, B. Unnikrishnan, Y.-J. Li, et al., *Biosensors and Bioelectronics*, 2015, **68**, 1-6.
56. X. Zhao, L. R. Hilliard, S. J. Mechery, Y. Wang, R. P. Bagwe, S. Jin, et al., *PNAS*, 2004, **101**, 15027-15032.
57. M. Magro, M. Zaccarin, G. Miotto, L. Da Dalt, D. Baratella, P. Fariselli, et al., *Analytical and Bioanalytical Chemistry*, 2018, **410**, 2949-2959.
58. G. Miotto, M. Magro, M. Terzo, M. Zaccarin, L. Da Dalt, E. Bonaiuto, et al., *Colloids and Surfaces B-Biointerfaces*, 2016, **140**, 40-49.
59. R. S. Samraj, B. Zingarelli and H. R. Wong, *Shock*, 2013, **40**, 358-365.
60. S. Schottler, K. Klein, K. Landfester and V. Mailander, *Nanoscale*, 2016, **8**, 5526-5536.
61. N. R. Stone, T. Bicanic, R. Salim and W. Hope, *Drugs*, 2016, **76**, 485-500.
62. R. Hamill, *Drugs*, 2013, **73**, 919-934.